

Frictional control of the phase separation of self-propelled particles

Pin Nie,^{1,2} Joyjit Chattoraj,¹ Antonio Piscitelli,^{1,3} Patrick Doyle,^{2,4} Ran Ni,^{5,*} and Massimo Pica Ciamarra^{1,3,†}

¹ *School of Physical and Mathematical Science, Nanyang Technological University, Singapore*

² *Singapore-MIT Alliance for Research and Technology, Singapore*

³ *CNR-SPIN, Dipartimento di Scienze Fisiche, Università di Napoli Federico II, I-80126, Napoli, Italy*

⁴ *Department of Chemical Engineering, Massachusetts Institute of Technology, Cambridge, Massachusetts, USA*

⁵ *School of Chemical and Biomedical Engineering, Nanyang Technological University*

(Dated: April 16, 2019)

Systems of self-propelled particles have the unique ability to phase separate, in the absence of any attractive interaction, into coexisting liquid and gas-like phases. The liquid clusters are highly dynamic, and continuously form and break through a mechanism attributed to the rotation of the self-propelling directions. Here we demonstrate that clusters might break through a novel instability mechanism induced by their rotational motion, and show that the efficiency of this mechanism is tamed by the frictional interaction between the particles. When this instability mechanism is present, phase separation only occurs if the density of the particles above a critical value, while conversely it occurs at all densities. The frictional dependence of this mechanism may thus allow to engineer the motility induced phase diagram by tuning the roughness of the particles.

Many biological and synthetic systems of self-propelled particles exhibit a transition from a homogeneous state to one in which a high-density liquid-like state coexists with a low-density gas-like state [1, 2]. While diverse physical processes might be responsible for the observed transition, the bare presence of motility is enough to induce it. Indeed, a motility induced phase separation (MIPS) is observed when the interaction between the particles is purely repulsive, and does not promote the alignment of the self-propelling directions. Under these conditions, the key to the observed phase separation is the coupling between the velocity of the particles and the local density, whereby particles are slower in a dense environment. The features of this transition have been rationalised when particles compete for the resources allowing for their motility, so that the active velocity is explicitly dependent on the local density. In this case [3], the transition from a homogenous to a phase separate state occurs at all values of the volume fraction of the active particles, provided that the activity is large enough. This is in strong analogy with the liquid-gas phase separation, if one identifies the motility strength as the inverse temperature. In many experimental and numerical realizations of active particles, however, the motility parameters do not explicitly depend on the density, and particles in dense environments are slower only because of crowding effects. When this is so, an increase in activity induces phase separation only if the volume fraction is above a critical value [4–7]. The physical origin of this critical volume fraction, whose existence marks a qualitative departure from the thermal case, is currently unknown. This lack of an understanding comes as a surprise, as crowding induced slowdown characterizes the active Brownian particles (ABPs) system, which is arguably the active particle model system that has been

investigated the most.

Here we demonstrate the existence of a previously unreported mechanism which makes a cluster of active particles unstable as it rotates. This instability mechanism is illustrated in Fig. 1a-d, where we report results from two dimensional simulations of smooth spherical ABPs (see Methods and below for details): as a cluster rotates the direction of the self-propelling forces become tangential to the cluster surface, making the cluster unstable. Building on a recent investigation of the rotational properties of clusters of active particles [8], we prove that this instability mechanism explains why in ABPs phase separation only occurs above a critical density. We further demonstrate that the efficiency of this instability mechanism can be tuned by acting on the strength of the frictional interaction between the particles (see Fig. 1a,e-g). In systems of active colloidal particles, this opens the possibility of experimentally controlling the features of the motility induced phase diagram by tuning the particle roughness.

Results

Effect of friction on MIPS for ABPs

We have investigated the motility induced phase diagram of self-propelled particles, and its dependence on the frictional interaction between the particles, focusing on the popular ABPs model (see Methods). We differ from the standard ABPs model only in the choice of the two-body interparticle interactions potential, which we borrow from the granular community. In our simulations, the force acting between two contacting particles has a normal and a tangential component. For the normal component, we use a one-sided Harmonic spring. We work in

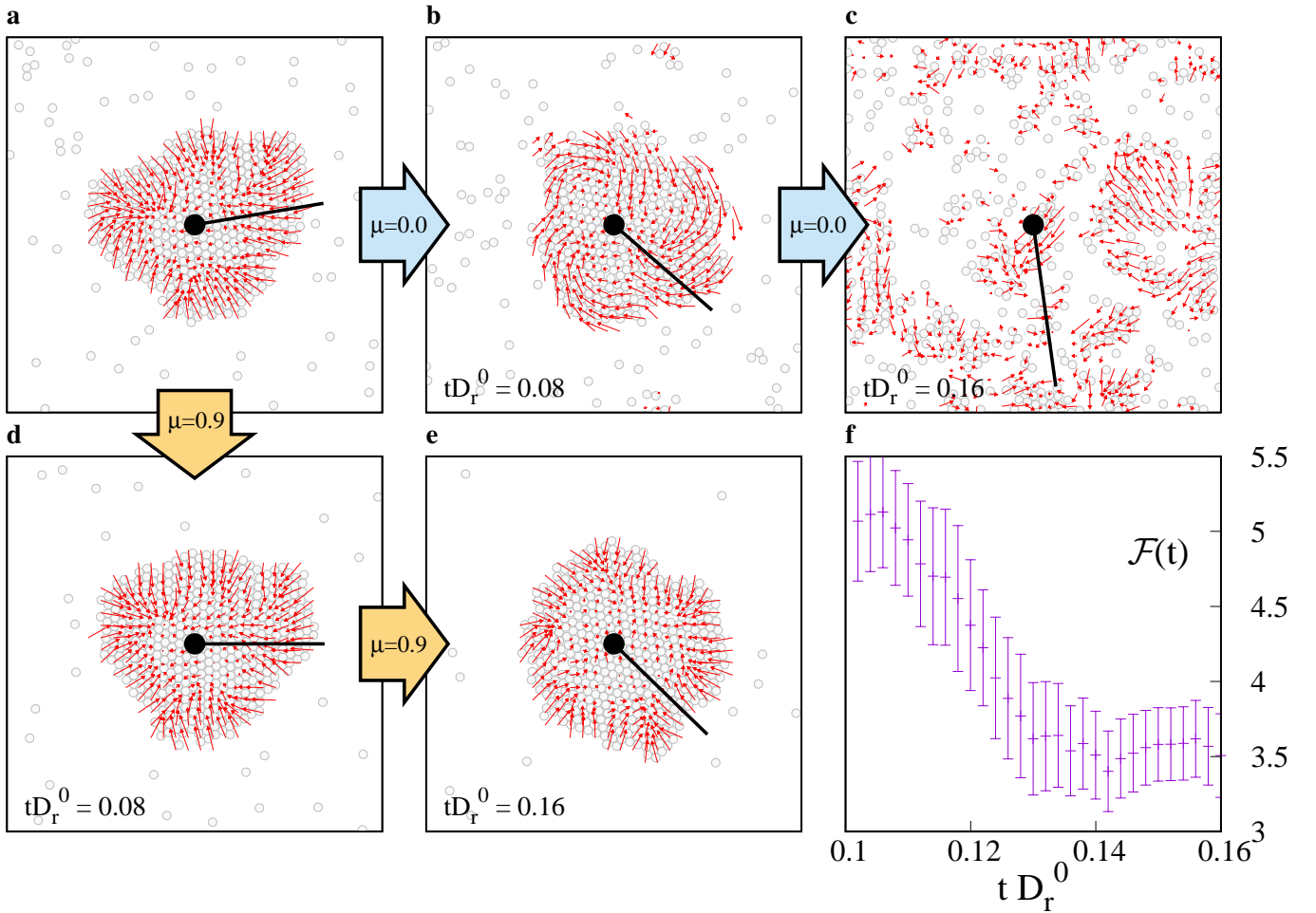


FIG. 1: Evolution of a two dimensional cluster of ABPs in the absence (**a,b,c**) and in the presence (**a,d,e**) of frictional forces. The red arrows show the active force field (see methods). In all plots, the central black circle identifies the position of the particle which is closer to the center of mass of the cluster, in the initial configuration. We emphasize the rotational motion of the cluster drawing a line connecting the central particle and another particle of the cluster. Both with and without friction the cluster rigidly rotates around its center of mass. In the absence of friction the rotation of the cluster makes the active velocities parallel to the cluster surface (**b**) inducing a cluster instability (**c**). Indeed, we see in panel **f** that, in the absence of friction, as the cluster rotates, the average interaction force that contrasts the motion along the direction of the self-propelling forces decreases, fluctuating around a value characteristic of the homogeneous phase once the cluster breaks. In the presence of friction the cluster rotation induces that of the self-propelling directions, and the cluster remains stable (**d,e**). For these illustrative two-dimensional simulations $N = 500$, $Pe = 500$, $\phi = 0.2$ and $\mu = 0.0; 0.9$.

the hard-sphere limit considering a large stiffness of the particles, which assures that the maximum relative deformation of a particle is $\leq 10^{-4}$ for the range of parameters we have considered. For the tangential interaction we have used the spring-dashpot model. The magnitude of the tangential force is bounded by the magnitude of the normal one by the Coulomb condition, $|\mathbf{f}^t| \leq \mu |\mathbf{f}^n|$, where μ is the friction coefficient. Thus, when $\mu = 0$ frictional forces are suppressed and our model reduces to the standard ABP model for stiff particles. Working in the overdamped limit, we neglect any viscous dissipation in the interparticle interaction. We have investigated the motility phase diagram as a function of the friction coefficient μ , of the volume fraction ϕ , and of the Peclet

number $Pe \equiv v_a \tau_B / \sigma$, where v_a is the particle velocity in the $\phi \rightarrow 0$ limit, σ the average particle diameter and $\tau_B = 1/D_r^0$ is the Brownian time, D_r^0 being the rotational diffusion coefficient of the self-propelling directions in the absence of friction. We have determined the phase diagram considering the systems to be phase separated when the distribution of the local density exhibits two peaks (see methods). Our system size ($N = 10^4$ if not otherwise specified) is large enough for finite size effect to be negligible on the location of this phase boundary (Supplemenray Fig. S1).

In the absence of friction, our results are in qualitative agreement with previous investigations. The increase of the Peclet number drives the phase separation of the

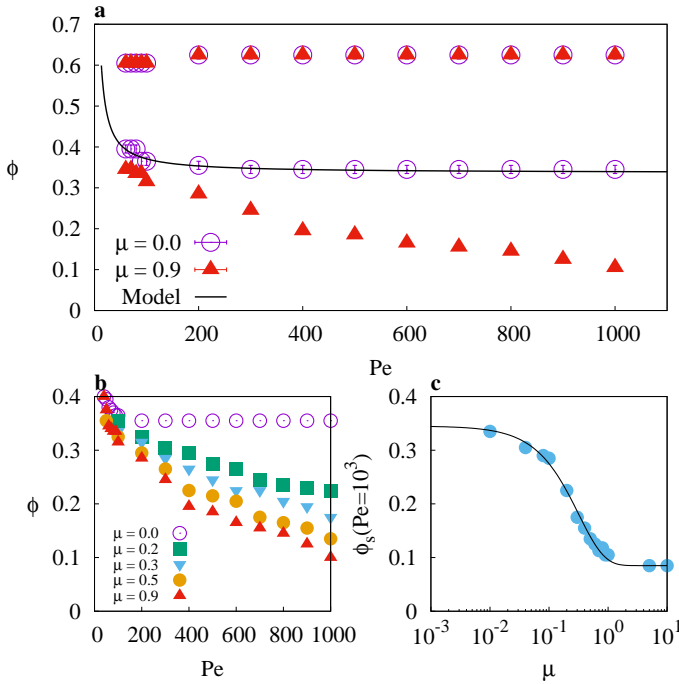


FIG. 2: The phase diagrams of frictionless (circles) and of frictional (triangles) ABPs are compared in (a). The full line corresponds to the theoretical prediction of Eq. 1. At high Pe the low density critical line saturates to a constant value in the absence of friction, while it vanishes in the frictional case. This occurs for all values of the friction coefficient, as shown in (b). At a given Pe , the critical volume fraction at which phase separation occurs varies with friction as $\phi_s(\mu) = \phi_s(\infty) + \Delta\phi_s e^{-\mu/\mu_c}$. For $Pe = 10^3$ (c) we find $\phi_s(\infty) = 0.085(3)$, $\Delta\phi_s = 0.26(2)$ and $\mu_c = 0.32(1)$.

system, but only if the volume fraction is larger than a critical value [4–7], as illustrated in Fig. 2a (circles). We rationalise the physical origin of this critical volume fraction, which is currently unknown, by extending the pioneering work by Redner et al. [9], who considered that the phase boundary is determined by the balance between the flux of particles j_{in} moving from the gas to the dense phase and the reverse flux of particles j_{out} . Previous results and dimensional analysis [3, 4, 9, 10] suggest $j_{in} = \alpha \rho_g v_a = \alpha Pe \rho_g \sigma / \tau_B$, where ρ_g is the number density of the gas phase, σ the average particle diameter, and α a geometric constant. To model j_{out} , previous works have considered that a particle on the surface of a cluster stick to it unless its self-propelling direction points away from the cluster. Hence, the rotation of the self-propelling directions of the particles on the surface of a cluster [3, 4, 9, 10] gives rise to a flux of particles from the dense to the gas phase. This flux scales as $j_{out}^{(1)} = k_0 D_r^0 \sigma^{-2}$ with k_0 a non-dimensional geometric constant, and D_r^0 the rotational diffusion coefficient of the particles. Since $j_{out}^{(1)}$ does not grow with Pe , while j_{in} does, by balancing j_{in} and $j_{out}^{(1)}$ one can predict the motil-

ity induced phase separation to occur at all volume fractions. This contradicts the numerical results [4–7], and indicates that there must be an additional escape mechanism, $j_{out}^{(2)}$. In the Supplementary Information (Fig. S2 and Animation 1) we show that active clusters break and rearrange when $j_{out}^{(1)}$ is set to zero by imposing $D_r^0 = 0$, both explicitly proving the existence of an additional escape mechanism, and demonstrating that this mechanism is not related to the rotational diffusion of the particles.

This novel cluster instability mechanism stems from the rotational motion of the active clusters. Indeed, as illustrated in Fig. 1a–c, a frictionless cluster becomes unstable and disintegrates upon rotation, as the cluster rotation makes the self-propelling velocities tangential to the cluster surface. We have verified that the system becomes macroscopically unstable by investigating the magnitude of the forces which opposes the motion of the particles along their self-propelling directions $\mathcal{F}(t) = -\frac{1}{N F_a} \frac{d}{d\alpha} U(\mathbf{r}(t) + \alpha \hat{\mathbf{n}})|_0$, where U is the elastic energy of the system and $\hat{\mathbf{n}}$ is the director of the active velocity field, normalized by the magnitude F_a of the active force acting on each particle and by the number of particles N . Fig. 1f shows that $\mathcal{F}(t)$ quickly decreases as the cluster rotates, reflecting the development of the instability. To estimate the outflux $j_{out}^{(2)}$ associated to this novel instability mechanism we build on a very recent investigation of the rotational dynamics of clusters of active spherical particles [8] and of active dumbbells [11, 12], that have clarified that their typical angular velocity scales as $\omega \propto \frac{1}{N_c} \frac{v_a}{\sigma} \propto \frac{1}{N_c} \frac{Pe}{\tau_B}$, where N_c is the number of particles of the cluster. Assuming that the rotation leads to the complete disintegration of the cluster, or equivalently to the escape of a finite fraction of the cluster particles, we find $j_{out}^{(2)} = k_1 \frac{Pe}{\tau_B} \sigma^{-2}$, with k_1 as a constant. By balancing j_{in} and $j_{out} = j_{out}^{(1)} + j_{out}^{(2)}$ we predict the following (low-density) phase boundary

$$\phi_s = k_0 \frac{D_r^0 \tau_B}{\alpha Pe} + \frac{k_1}{\alpha} = \frac{\beta}{Pe} + \phi_c, \quad (1)$$

where β and ϕ_c are unknown constants, the latter representing the minimum volume fraction for phase separation to occur. Fig. 2 shows that this theoretical prediction well describes the numerical data. We remark that a finite ϕ_c is the consequence of the proportionality between $j_{out}^{(2)}$ and j_{in} , which both scale with the Peclet number. Let us also mention that we have described the new instability mechanism assuming the rotational velocity of a cluster to be constant. This approximation holds as, at large Pe , the instability mechanism takes place well before the time $\sim 1/D_r^0$ at which the angular velocity of the cluster would decorrelate, as apparent in Fig. 1f.

The reported instability mechanism is at work when the rotation of a cluster does not induce that of the self-propelling directions of its particles, as in systems of spherical ABPs. On the contrary, this instability mecha-

nism is suppressed. This occurs, for instance, in systems of rod-shaped particles such as active dumbbells. Indeed, clusters of active dumbbells perform long-lived rotations and active dumbbells phase separate at all volume fractions [11, 12]. This suggests the possibility of tuning the novel instability mechanism which we have reported by acting on the frictional interaction between the particles [12], certainly present in experimental dry active matter and possibly at work in colloidal (wet) active matter. Indeed, while direct interparticle interactions in a fluid are generally screened by a fluid layer trapped in between the colliding particles, it has been recently demonstrated that direct frictional interparticle contacts do actually occur in colloidal suspensions under shear, giving rise to the discontinuous shear thickening phenomenology [13–16]. Accordingly, frictional forces may be in principle at work in thermophoretic active particles [10, 17, 18], or might be engineered to become relevant [15].

We have investigated the possibility of tuning the motility induced phase diagram acting on the roughness of the particles by performing simulations of frictional ABPs for different values of the friction coefficient. Fig. 2a compares the frictionless (circles) and the frictional (triangles) phase diagram, and reveals that in the presence of friction phase separation occurs at all volume fractions provided that the Peclet number is high enough. This is confirmed in Fig. 2b, where we illustrate that in the presence of friction the low-density transition lines continuously decrease as the Peclet number increases. We further investigate the effect of friction in Fig. 2c, showing that at a fixed value of the Peclet number the phase transition occurs at a volume fraction exponentially approaching a limiting value as the friction coefficient increases. This limiting value decreases as the Peclet number increases. Physically, the saturation at high μ is rationalised considering that an increase in the friction coefficient does not influence the dynamics if μ is so large that no contact reaches the Coulomb threshold. A similar effect of friction has been reported on the volume fraction of static granular packing [19].

We rationalise how friction modifies the motility induced phase diagram focusing on its effects on the fluxes of particles joining and leaving an active cluster. To evaluate the effect of friction on the flux of particles joining an active cluster we compare in Fig. 3a, the frictionless and the frictional mean square displacement at different Peclet numbers, for volume fractions in the gas phase. In the absence of friction (full lines) the mean square displacement exhibits the expected crossovers from a diffusive to a super-diffusive regime at $t \simeq 6D_t^0/v_a^2$, and from the super-diffusive to the asymptotic diffusive regime at $t = 1/D_r^0$ [9]. In the presence of friction (symbols) a similar behaviour is observed, but the time scale at which the system enters the diffusive regime is reduced. Consequently, as illustrated in 3b, the translational diffu-

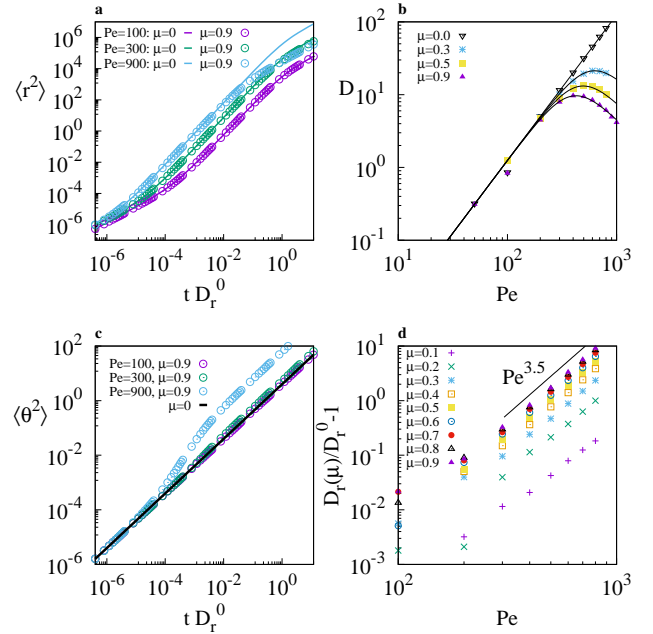


FIG. 3: Mean square displacement (a) for the frictionless ($\mu = 0$, full lines) and the frictional dynamics ($\mu = 0.9$, symbols) for selected values of the Peclet number. At large Pe friction reduces the time at which the dynamics enters the asymptotic diffusive regime, and hence suppresses the diffusion coefficient (b). The mean square angular displacement (c) is enhanced by the frictional force, at times larger than the interparticle collision time. This leads to an increase of the rotational diffusivity (d) scaling as $\mu^2 Pe^x$, with $x \simeq 3.5$. Lines in (b) are one parameter fits to the theoretical prediction of Eq. 3 where $x = 3.5$ is held constant. In all panels, $\phi = 0.1$.

sivity is also reduced. This is rationalised investigating the mean square angular displacement (3c) and the dependence of the rotational diffusivity D_r on Pe (3d). Indeed, these quantities clarify that friction enhances the rotational diffusion of the particles, hence reducing the timescale at which the system enters the asymptotic translational diffusive regime. This occurs as during a collision a frictional particle experiences a torque, which induces the rotation of its self-propelling direction.

More quantitatively, in the overdamped limit the rotation $\Delta\theta_i$ induced by a collision is proportional to the induced torque, and to the duration of the contact. Assuming the contacts to be at their critical Coulomb value, the typical torque magnitude is $\sigma f^t \propto \mu f^n \propto \mu Pe$, and the mean squared angular displacement induced by a collision of duration t_{coll} is $\langle \Delta\theta_i^2 \rangle \propto \mu^2 Pe^2 t_{\text{coll}}^2$. At low density consecutive torques experienced by a particle are uncorrelated and the number of collisions per unit time is proportional to Pe . Hence, assuming $t_{\text{coll}} \propto Pe^q$, we

predict for the rotational diffusivity

$$D_r(\text{Pe}, \mu) = D_r^0 + \alpha \mu^2 \text{Pe}^x \quad (2)$$

with $x = 3 + 2q$. Our numerical results of Fig. 3d indicate $x \simeq 3.5$. Thus, the average duration of an interparticle collision slightly grows with the Peclet number, $t_{\text{coll}} \propto \text{Pe}^{1/4}$ (see Supplementray Fig. S3). The dependence of the rotational diffusion coefficient on Pe and on μ allows also to rationalise the non monotonic behaviour of the diffusivity observed in Fig. 3b. Indeed, in the $\phi \rightarrow 0$ limit the long time mean square displacement of an active particle is $\Delta r^2(t) = 6D_t^0 t + \frac{v_a^2}{D_r} t$, so that at low density we expect

$$D(\text{Pe}, \mu) = c(\phi) \left[D_t^0 + \frac{\sigma^2}{6} \frac{(D_r^0)^2}{D_r(\text{Pe}, \mu)} \text{Pe}^2 \right] \quad (3)$$

with $c(\phi)$ a constant of order unit. This well describes the data of Fig. 3b, with $c(\phi = 0.1) \simeq 0.8$. Hence, the diffusivity grows as Pe^2 at small Pe, and decreases as Pe^{2-x} at large Pe.

These results clarify that in the gas phase the effect of friction on the dynamics is only apparent at long times, as it is the cumulative effect of many frictional collisions to induce a change in the diffusivity. It is therefore safe to assume that friction does not affect the flux j_{in} of gas particles joining a close-by cluster. In addition, the dependence of the rotational diffusion on the friction coefficient clarifies that friction affects the dynamics when the Peclet number overcomes a threshold $\text{Pe}^*(\mu) \propto \mu^{-4/7}$. Indeed, we show in Fig. 4a that, when plotted vs Pe/Pe^* , rotational diffusivity data corresponding to different values of the friction coefficient nicely collapse. The threshold Pe^* signifies that friction is only relevant when the frictional forces are strong enough with respect to the thermal ones.

While friction does not influence the flux of particles joining an active cluster from the gas phase, it strongly affects the reverse flux $j_{\text{out}} = j_{\text{out}}^{(1)} + j_{\text{out}}^{(2)}$. The outflux $j_{\text{out}}^{(1)}$, which originates from the rotational motion of the particles on the cluster surface, is suppressed as these particles are no longer free to rotate their self-propelling directions. More quantitatively, the energy needed to rotate a particle by an angle θ scales as $\Delta E \propto F_t \theta \sigma \propto \mu F_n \theta \sigma \propto \mu \tau_B^{-1} \eta \sigma^2 \text{Pe}$ where we have considered that in the overdamped limit the typical force acting on the particle is the self-propelling force $v_a \eta$ in a solvent with viscosity η . Thus, while with no friction $\Delta E = 0$ and the physical process leading to the outflux $j_{\text{out}}^{(1)}$ is diffusive, in the presence of friction the same process is an activated one and is therefore strongly suppressed, at least at large Pe. Friction also affects the flux $j_{\text{out}}^{(2)}$ resulting from the rotational instability of the clusters. Indeed, at high Pe contacts within a cluster do not break due to thermal fluctuations, so that in the presence of friction the rotation of the cluster implies the rotation of the

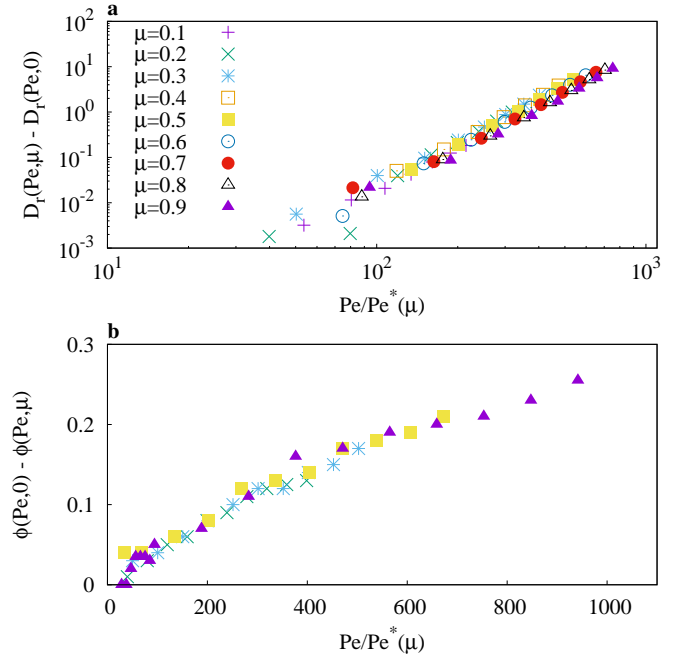


FIG. 4: Friction leads to an increase of the rotational diffusivity scaling as $D_r(\text{Pe}, \mu) - D_r(\text{Pe}, 0) \propto \text{Pe}^* \propto \mu^{-4/7}$ (a). The difference between the frictionless and the frictional low density critical lines (see Fig. 2b) is also controlled by Pe^* (b).

self-propelling directions of its particles, as illustrated in Fig. 1a,e-g. This suppresses $j_{\text{out}}^{(2)}$.

The above results allow to quantitatively rationalise the influence of friction on the motility induced phase diagram. Indeed, friction affects the dynamics when the frictional forces become comparable to the thermal ones, we have seen to occur at a Peclet number scaling as $\text{Pe}^*(\mu) \propto \mu^{-4/7}$. Accordingly, the frictional critical line $\phi_c(\text{Pe}, \mu)$ coincides with the frictionless one for $\text{Pe} < \text{Pe}^*(\mu)$, while conversely it deviates from it. We confirm this expectation in Fig. 4b, which illustrates that the distance between the frictionless and the frictional critical lines, $\phi(\text{Pe}, 0) - \phi_c(\text{Pe}, \mu)$ scales as $\text{Pe}/\text{Pe}^*(\mu)$.

Discussion

We have demonstrated that clusters of active particles may become unstable through a previously unreported mechanism which is driven by their rotational motion. This novel instability mechanism allows to quantitatively rationalise the phase diagram of active Brownian particles and explains why their motility induced phase transition only occurs above a critical volume fraction value. This instability mechanism is suppressed in the presence of a strong coupling between the rotational motion of an active cluster and that of its particles. This coupling occurs in systems of anisotropic active particles, which cannot rotate independently, and that phase sep-

arates at all volume fractions [11, 12]. Similarly, this mechanism is suppressed in Monte Carlo based simulations of active particles [20, 21], as this simulation technique suppresses collective particle displacements. Interestingly, we have clarified that it is possible to smoothly affect the efficiency of this instability mechanism by acting on the frictional interaction of the particles. This suggests that it is possible to modulate the features of the motility induced phase diagram by engineering the roughness of the particles. In this respect, friction appears to play a similar role in active and in passive colloidal systems [15]. We conclude by speculating that friction could be already at work in experiments of thermophoretic particles, where one observes long-lived rotating clusters [10, 17, 18]. These clusters might perform several revolutions before restructuring, which is not the case in frictionless ABPs due to the instability mechanism we have discussed. While it is understood that these clusters might be stabilised by the attractive phoretic attraction between the particles [17, 18, 22], it has been suggested that this is not always present [10]. In these circumstances friction might be a concurring stabilising factor, as one could experimentally ascertain investigating whether the self-propelling directions of the particles rotate with the cluster itself.

Methods

We consider two and three dimensional suspensions of active spherical Brownian particles (ABPs) with average diameter σ (polydispersity: 2.89%) and mass m , in the overdamped limit. The equations of motion for the translational and the rotational velocities are

$$\mathbf{v}_i = \frac{\mathbf{F}_i}{\gamma} + \frac{F_a}{\gamma} \hat{\mathbf{n}}_i + \sqrt{2D_t^0} \boldsymbol{\eta}_i^t \quad (4)$$

$$\boldsymbol{\omega}_i = \frac{\mathbf{T}_i}{\gamma_r} + \sqrt{2D_r^0} \boldsymbol{\eta}_i^r. \quad (5)$$

Here D_r^0 and $D_t^0 = D_r^0 \sigma^2 / 3$ are the rotational and the translational diffusion coefficients, $\gamma_r = \gamma \frac{\sigma^2}{3}$, η is Gaussian white noise variable with $\langle \eta \rangle = 0$ and $\langle \eta(t) \eta(t') \rangle = \delta(t - t')$, F_a the magnitude of the active force acting on the particle and $\hat{\mathbf{n}}_i$ its direction, $\mathbf{F}_i = \sum \mathbf{F}_{ij}$ and $\mathbf{T}_i = \frac{\sigma_i}{2} \sum (\hat{\mathbf{r}}_{ij} \times \mathbf{F}_{ij})$ are the forces and the torques arising from the interparticle interactions. In absence of interaction and noise, particles move with velocity $\mathbf{v}_a = F_a / \gamma$, and does not rotate.

We use an interparticle interaction model borrowed from the granular community, to model frictional particles. The interaction force has a normal and a tangential component, $\mathbf{F}_{ij} = \mathbf{f}_{ij}^n + \mathbf{f}_{ij}^t$. The normal interaction is a purely repulsive Harmonic interaction, $\mathbf{f}_{ij}^n = k_n(\sigma_{ij} - r_{ij})\Theta(\sigma_{ij} - r_{ij})\hat{\mathbf{r}}_{ij}$, $\Theta(x)$ is the Heaviside function, $\sigma_{ij} = (1/2)(\sigma_i + \sigma_j)$, $\mathbf{r}_{ij} = \mathbf{r}_i - \mathbf{r}_j$, and \mathbf{r}_i is the

position of particle i . The tangential force is $\mathbf{f}_{ij}^t = k_t \vec{\xi}_{ij}$, where ξ_{ij} is the shear displacement, defined as the integral of the relative velocity of the interacting particle at the contact point over the duration of the contact, and $k_t = \frac{2}{7}k_n$. In addition, the magnitude of tangential force is bounded according to Coulomb's condition: $|\mathbf{f}_{ij}^t| \leq \mu |\mathbf{f}_{ij}^n|$. The value of k_n is chosen to work in the hard-sphere limit, the maximum deformation of a particle being of order $\delta/\sigma \leq 5 \times 10^{-4}$. Simulations [23] are done integrating the equation of motion via the overdamped Langevin algorithm, with integration timestep $2 \times 10^{-8} / D_r^0$. The number of particles is $N = 10^4$, unless stated otherwise. Finite size effects for the three dimensional simulations have been investigated considering values of N up to 10^5 , as in the supporting material. All data are collected after discarding a preliminary run lasting at least 2τ , where τ is the time at which the diffusive regime is attained. We use σ , m and $\sqrt{m/k_n}$ as our units of length, mass and time.

We determine the critical lines investigating the emergence of bimodality in the distribution $P(\phi_L)$ of the local volume fraction. We measure ϕ_L in cubic boxes of side length corresponding to twice the average interparticle separation $2\rho^{-1/d}$, in d spatial dimensions. This choice assures that $P(\phi_L)$ is single peaked in the absence of phase separation.

The active velocity field in Fig. 1 is evaluated on a square grid with lattice spacing $\sim 1.5\sigma$. We associate to each grid point the average active force of the particles in a circle of radius $\simeq 2.2\sigma$. In the figure we show the values of the field on the grid points that average over at least 5 particles.

* Electronic address: r.ni@ntu.edu.sg

† Electronic address: massimo@ntu.edu.sg

- [1] M. C. Marchetti, J. F. Joanny, S. Ramaswamy, T. B. Liverpool, J. Prost, M. Rao, and R. A. Simha, *Rev. Mod. Phys.* p. 1143 (2013).
- [2] C. Bechinger, R. D. Leonardo, C. Reichhardt, G. Volpe, and G. Volpe, *Rev. Mod. Phys.* **88**, 045006 (2016).
- [3] M. E. Cates and J. Tailleur, *The Annual Review of Condensed Matter Physics* is *Annu. Rev. Condens. Matter Phys.* **6**, 219 (2015).
- [4] A. Wysocki, R. G. Winkler, and G. Gompper, *EPL (Europhysics Letters)* **105**, 48004 (2014).
- [5] J. Stenhammar, D. Marenduzzo, R. J. Allen, and M. E. Cates, *Soft Matter* **10**, 1489 (2014).
- [6] D. Levis, J. Codina, and I. Pagonabarraga, *Soft Matter* **13**, 8113 (2017).
- [7] P. Digregorio, D. Levis, A. Suma, L. F. Cugliandolo, G. Gonnella, and I. Pagonabarraga, *Physical Review Letters* **121** (2018).
- [8] F. Ginot, I. Theurkauff, F. Detcheverry, C. Ybert, and C. Cottin-Bizonne, *Nature Communications* **9**, 696 (2018).
- [9] G. S. Redner, M. F. Hagan, A. Baskaran, and M. Fisher,

- Phys Rev Lett **110**, 055701 (2013).
- [10] I. Buttinoni, J. Bialké, F. Kümmel, H. Löwen, C. Bechinger, and T. Speck (2013).
 - [11] A. Suma, G. Gonnella, D. Marenduzzo, and E. Orlandini, EPL (Europhysics Letters) **108**, 56004 (2014).
 - [12] I. Petrelli, P. Digregorio, L. F. Cugliandolo, G. Gonnella, and A. Suma, European Physical Journal E p. 128 (2018).
 - [13] B. M. Guy, M. Hermes, and W. C. K. Poon, Phys Rev Lett **115**, 088304 (2015).
 - [14] C. Clavaud, A. Bérut, B. Metzger, and Y. Forterre, Proceedings of the National Academy of Sciences of the United States of America **114**, 5147 (2017).
 - [15] C.-P. Hsu, S. N. Ramakrishna, M. Zanini, N. D. Spencer, and L. Isa, Proceedings of the National Academy of Sciences of the United States of America **115**, 5117 (2018).
 - [16] T. Kawasaki and L. Berthier, Physical Review E **98**, 012609 (2018).
 - [17] I. Theurkauff, C. Cottin-Bizonne, J. Palacci, C. Ybert, and L. Bocquet, Physical Review Letters p. 268303 (2012).
 - [18] J. Palacci, S. Sacanna, A. P. Steinberg, D. J. Pine, and P. M. Chaikin, Science **339**, 936 (2013).
 - [19] L. E. Silbert, Soft Matter **6**, 2918 (2010).
 - [20] D. Levis and L. Berthier, Physical Review E **89**, 62301 (2014).
 - [21] J. U. Klamser, S. C. Kapfer, and W. Krauth, Nature Communications **9**, 5045 (2018).
 - [22] B. Liebchen and H. Löwen, J. Chem. Phys **150**, 61102 (2019), URL <https://doi.org/10.1063/1.5082284>.
 - [23] S. Plimpton, J. Comput. Phys. **117**, 1 (1995).